IJE TRANSACTIONS B: Applications Vol. 39, No. 08, (August 2026) 1790-1801

International Journal of Engineering

Journal Homepage: www.ije.ir

Effect of Different Non-aqueous Phase Liquids on Geoenvironmental Properties of Sandy Soils Stabilized with Bentonite

H. Tamadon Ghareghieh[a], M. Yazdi*[a], D. Yousefi Kebria[b], H. Aminirad[b]

[a] *Department of Civil Engineering, CT.C., Islamic Azad University, Tehran, Iran*
[b] *Environmental Engineering Department, Faculty of Civil Engineering, Babol Noshirvani University of Technology, Babol, Iran*

PAPER INFO

Paper history:
Received 01 July 2025
Received in revised form 14 August 2025
Accepted 27 August 2025

Keywords:
Soil Microstructure Analysis
Non-aqueous Phase Liquid Contamination
Bentonite-Amended Sandy Soil
Geoenvironmental Engineering
Hydraulic and Shear Behavior

ABSTRACT

Energy requirements for remediation of petroleum-contaminated soils and strategy selection are essential from both environmental and geotechnical perspectives. The effectiveness of clay minerals and other stabilizers in enhancing the geotechnical properties of sandy soils contaminated with light non-aqueous phase liquids (LNAPLs) was confirmed in previous research. However, the combined impact of bentonite to sand ratio (BSR), and type and concentration of LNAPL simultaneously on geotechnical and environmental properties has not been thoroughly investigated and remains poorly understood. In this study, the influence of diesel and benzene with different concentrations (100, 150, 200, and 250 g LNAPLs/kg dry soil) on the geoenvironmental characteristics of sandy soils stabilized and improved using different BSRs (0, 0.2, 0.4, and 0.6) were comperehesllly evaluated. The results indicated an increase in maximum dry density (MDD) and a reduction in optimum moisture content (OMC) during the compaction tests. Additionally, a decrease in cohesion and a decrease in the friction angle were observed in soils with higher concentrations of LNAPLs and BSR, with diesel exhibiting more pronounced effects than benzene. An increase in MDD and a decrease in OMC were also noted with escalating concentrations of both LNAPLs. Based on the results, BSR = 0.4 was found to be the optimal value that the soil mixture exhibits high MDD, low permeability (1×10^{-9}–7×10^{-9} cm/s), significantly increased cohesion (>50 kPa), and acceptable internal friction angles (~20–22°), at the concentrations of 150–200 g/kg. Analytical techniques, including FTIR, EDAX, XRF, and XRD were confirmed these results, providing insights into the mechanisms of contaminant retention in bentonite-amended sandy soils. The findings of this study can inform the geotechnical design of structures on LNAPL-contaminated soils and guide the selection of appropriate remediation methods.

***doi**: 10.5829/ije.2026.39.08b.01*

Graphical Abstract

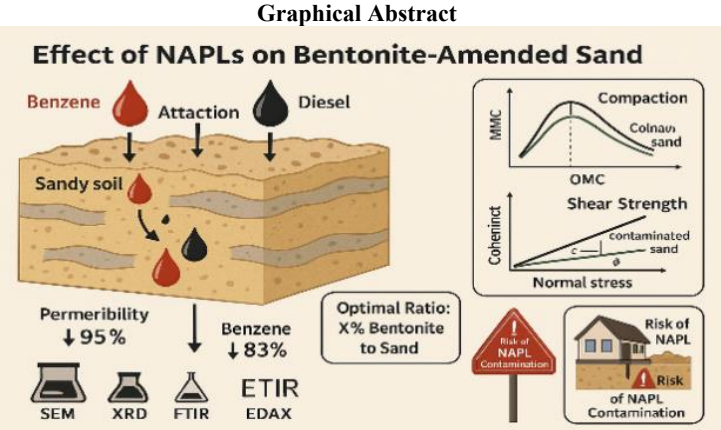

* Corresponding Author Email: mar.yazdi@iau.ac.ir (M. Yazdi)

Please cite this article as: Tamadon Ghareghieh H, Yazdi M, Yousefi Kebria D, Aminirad H. Effect of Different Non-aqueous Phase Liquids on Geoenvironmental Properties of Sandy Soils Stabilized with Bentonite. International Journal of Engineering, Transactions B: Applications. 2026;39(08):1790-801.

1. INTRODUCTION

Soil contamination by petroleum hydrocarbons in coastal sandy areas, as highlighted in various studies and reports by the USEPA and UN environmental programs, poses significant environmental risks and challenges for civil engineering projects. Remediation of petroleum-contaminated sandy soils via thermal desorption methods typically requires up to 5,000–6,000 kJ/kg (1.4–1.7 kWh/kg), while electrochemical methods have reported specific energy consumption in the range of 1.6–2.9 kWh/kg, depending on contamination levels and scale (1, 2).

Recent studies have supported the efficacy of bentonite-enhanced bioremediation observed by Adams et al. (3). TPH concentration was reduced by approximately 55% after 28.8 months. However, Qv et al. (4) demonstrated that adding bentonite to aerobic composting of petroleum-contaminated soil improved hydrocarbon removal efficiency from 45% to 79%. Similarly, Li et al. (5) confirmed that advanced oxidation processes combined with mineral additives significantly enhanced hydrocarbon degradation, aligning with the stabilization trends reported in earlier field-scale studies.

Improving the geoenvironmental properties of these soils is crucial to ensure both environmental safety and structural stability in infrastructure development. Light Non-Aqueous Phase Liquids (LNAPLs), such as diesel and benzene with different Physicochemical characteristics, are among the most pervasive organic pollutants adversely affecting groundwater and soil systems on a global scale (6). Due to their low water solubility and high hydrophobicity, LNAPLs tend to persist in the subsurface environment, leading to long-term pollution and posing Substantial risks to human health and ecosystems (7, 8). Sandy soils, w ith large pore spaces and high permeability, facilitate rapid LNAPL migration, which complicates remediation methods and increases the potential for widespread contamination (9). Consequently, improving the geotechnical and geoenvironmental characterization of sandy soils to limit contaminant migration has become an essential research concern.

Sandy soil stabilization using bentonite with high swelling capacity and cation exchange capacity has been widely adopted as an effective method to enhance geoenvironmental engineering properties (10, 11), because it is enable to fill soil voids, adsorb NAPLs, and reduce contaminant migration (12, 13).

Physical and biochemical remediation of petroleum hydrocarbons contaminated soil, as well as the use of bentonite as a stabilization agent to stabilize the sandy soil contaminated with NAPLs, has been widely investigated and reported by our group, which has shown promising results in enhancing soil remediation and stabilization methods and reducing leaching of contaminated fields (14-19). Furthermore, Several studies have demonstrated that bentonite amendments can significantly enhance soil cohesion and decrease hydraulic conductivity, providing both structural reinforcement and environmental containment (20-22).

Also, statistical and numerical modeling have been used in related studies. De Medeiros et al. (22) used ANOVA to evaluate the influence of moisture content and emulsion type on the stiffness of stabilized soil and found that moisture content and emulsion type significantly affect soil stiffness, with certain emulsions performing best at optimal moisture. Zheng et al. (23) employed numerical modeling and showed that a confined sand cell reduces vibration transmission and improves damping. Kassem et al. (24) reported that cemented phosphogypsum enhances strength and durability, especially under cyclic loading.

Moreover, most other investigations have focused on either geotechnical improvements or contaminant adsorption separately, with limited integrated analysis of how LNAPL contamination influences the mechanical and environmental behavior of bentonite-stabilized sandy soils (25). For example, Safehian et al. (26) showed that increasing diesel concentration (from 100 to 250 g /kg dry soil) in fine-grained soil resulted in a decrease in maximum dry density (MDD), uniaxial strength, internal friction angle, and cohesion, while increasing compressibility and OMC. Similarly, the results of Al-Aghbari et al. (27)demonstrate that the Atterberg limits and cohesion of sandy soils contaminated with diesel fuel and gasoline (at concentrations of 0%, 5%, and 10%) were enhanced, while the angle of internal friction, permeability, and OMC were reduced. These findings aligned with Nasehi et al. (28), who Indicated a decrease in MDD, OMC, and internal friction angle, while cohesion and Atterberg limits increased in fine-grained soil.

Hanaei et al. (29) investigated the effect of varying contamination levels (0%, 5%, 10%, and 15%) of diesel and benzene on two types of sandy soils. The results revealed a reduction in permeability of the contaminated soils, as well as a decline in MDD and OMC. Moreover, direct shear tests showed increased cohesion and decreased internal friction angle following contamination.

To comprehensively evaluate the impact of LNAPL contamination on the engineering and chemical behavior of bentonite-stabilized sandy soils, this research employed several advanced characterization experiments, including Fourier Transform Infrared Spectroscopy (FTIR), Energy Dispersive X-ray Spectroscopy (EDX), X-Ray Fluorescence (XRF), and X-Ray Diffraction (XRD) were used to explain the microstructural and chemical modifications and

interaction between LNAPLs and soils. Moreover, the synergistic effects and coupled impacts of type and concentration of LNAPL, and bentonite content (BSR) on geotechnical and environmental behavior were assessed to determine the optimal BSR that balances practical and economic factors. Because too much bentonite can reduce soil structure or increase costs without sufficient benefits.

2. MATERIALS AND METHODS

2. 1. Sand-Bentonite Mixture The sandy soil was collected from the southern coastline of the Caspian Sea (Iran). The particle size distribution was determined in accordance with ASTM D422 (30). The specific gravity was measured to be 2.75 g/cm³, following the procedures outlined in ASTM D854 (31). According to the results of grain size analysis and the Unified Soil Classification System (USCS), the sand and bentonite samples were classified as SP (poorly graded sand) and CH (clay with high plasticity), respectively. To identify the dominant mineralogical composition of the bentonite, XRD analysis was performed using a diffractometer equipped with Cu-Kα radiation (λ = 0.154 nm). The analysis revealed montmorillonite as the primary clay mineral. Additionally, quartz, clinoptilolite, cristobalite, and calcite were identified as minor constituents (see Figure 1). The key physical properties of the sand and bentonite used in this study are summarized in Table 1.

Furthermore, Table 2 presents the chemical composition of both materials, as determined through XRF analysis. To ensure homogeneity across all test specimens, the required soil quantities were first sieved through a No. 4 mesh and subsequently oven-dried at 105 °C for 24 hours. Diesel and benzene—procured from the Tehran Oil Refinery—were selected as the representative petroleum-based contaminants due to their widespread presence in petroleum-contaminated soils globally and in the Caspian coastal region, as documented by the U.S. Environmental Protection Agency (USEPA) in large-scale spill assessments.

The dried soil was then mixed with sodium bentonite at different BSRs (0, 0.2, 0.4, and 0.6), and separately contaminated different concentrations of diesel and benzene (100, 150, 200, and 250 g /kg dry soil), following the approach by Sarmadi et al. (32). The applied concentrations with observed TPH ranges reported in sediments and soils affected by major spills.

To achieve uniform distribution and stabilization of the mixtures, the prepared samples were conditioned at at standard laboratory ambient temperature, assumed to be approximately 25 °C (33).

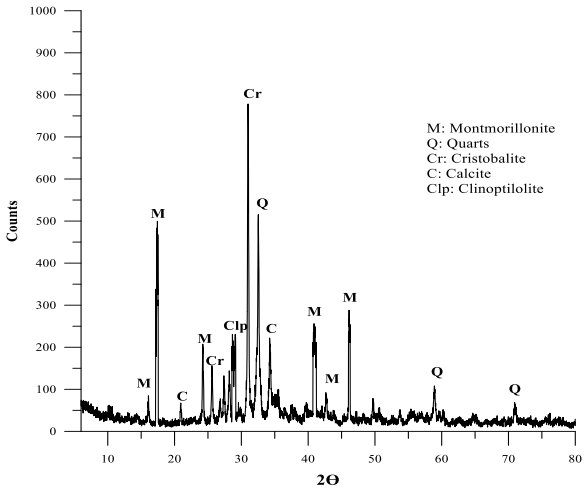

Figure 1. XRD pattern of bentonite

TABLE 1. Parameters of soil characteristics

Parameter	Sand	Bentonite
Classification (USCS)	SP	CH
Specific gravity (*Gs*)	2.75	2.7
Liquid Limit (%)	-	135
Plastic Limit (%)	-	40
Plasticity Index (%)	-	95
Maximum dry density (gr/cm^3)	1.77	1.48
Minimum dry density (gr/cm^3)	1.5	1.31
D_{50} (mm)	0.22	-
e_{min}	0.53	-
e_{max}	0.8	-
C_u	1.6	
C_s	1.1	

TABLE 2. Element Data of sand and bentonite sample

Soil	Compound (%)											
	SiO_2	Al_2O_3	Fe_2O_3	TiO_2	CaO	MgO	Na_2O	K_2O	SO_3	MnO	P_2O_5	LOI
Sand	93.5	0.82	1.26	-	1.43	0.223	0.061	0.095	0.27	-	-	1.04
Bentonite	61.4	13	2.5	0.25	4.7	1.24	2.7	0.6	0.45	0.04	0.07	12

2. 2. Methods A comprehensive suite of experimental procedures was employed to evaluate the geotechnical and chemical characteristics of the contaminated and treated soil specimens. Standard Proctor compaction tests, conducted in accordance with ASTM D698 (34), were used to determine the MDD and OMC of each soil mix. Shear strength parameters, including cohesion and internal friction angle, were obtained through direct shear tests following the ASTM D3080 (35) standard. To evaluate the hydraulic behavior of the specimens, constant head permeability tests were performed in line with ASTM D2434(36). In addition to mechanical characterization, the chemical alterations induced by hydrocarbon contamination and bentonite treatment were assessed using FTIR, conducted in accordance with ASTM D5477 (37). This integrative testing approach enabled a robust analysis of the physical, hydraulic, and chemical response of the sand–bentonite mixtures under varying contaminant levels.

2. 2. 1. Compaction Test Each sample was prepared using a cylindrical mold with a diameter of 4 inches and an approximate volume of 945 cm³. The soil was placed in five equal layers, and each layer was compacted by applying 25 uniform blows using a 10-pound hammer dropped from a height of 18 inches. Upon completion of compaction, the specimens' dry densities and moisture contents were determined. For hydrocarbon-contaminated specimens, the moisture content was calculated using a modified approach that accounts for the residual hydrocarbons present after drying, as proposed by Khamehchiyan et al. (38). The calculation is expressed by Equation 1:

$$W(\%) = (1 + mn)\frac{\mathrm{Wt}}{\mathrm{Wd}} - (1 + n) \quad (1)$$

where W_t is Weight of the moist contaminated soil, W_d is Weight of the dry contaminated soil, m is Percentage of residual contaminant after drying and n (%) is Initial percentage of contaminant before drying.

This correction ensures accurate determination of water content in samples where hydrocarbons may evaporate or partially remain during the drying process.

2. 2. 2. Direct Shear Test Direct shear tests were carried out in accordance with ASTM D3080 (39) to determine the shear strength parameters of the soil Mixture, specifically the internal friction angle (ϕ) and cohesion (c). A direct shear apparatus equipped with a shear box of dimensions 100 × 100 mm² was utilized for this purpose. Specimens were compacted into the shear box in three to four uniform layers using Plexiglas frames, each with dimensions of 10 cm × 10 cm × 3.3 cm, to ensure the final specimen volume matched the box capacity. The compaction was performed at the OMC corresponding to the previously determined MDD of each mix. Shear testing was conducted under constant normal stresses of 50, 100, 150, 200, and 250 kPa, with a controlled horizontal displacement rate of 0.7 mm/min. This setup allowed for accurate determination of the stress–strain behavior and failure envelopes of the contaminated and treated soil specimens.

2. 2. 3. Permeability Test Constant head permeability tests were performed in accordance with ASTM D2434 (36) to evaluate the hydraulic conductivity of the soil specimens. To enhance the accuracy of the results, each test was repeated three times per specimen, and the average value was recorded as the final result. The testing apparatus included a cylindrical mold with an internal diameter of 8 cm and a height of 22 cm. Hydraulic conductivity (K) in the vertical direction was calculated using the following equation:

$$K = \frac{Q \times L}{t \times A \times h} \quad (2)$$

where Q is volume of water discharged, L is length of the soil specimen, t: Duration of flow, A is cross-section area of the soil specimen and h is constant head.

2. 2. 4. FTIR Analysis Fourier Transform Infrared Spectroscopy (FTIR) analyses were conducted in accordance with ASTM D5477 (37) and ASTM E168-16 (39) to investigate chemical interactions and changes in functional groups within the soil specimens. The FTIR technique detects molecular vibrations, including stretching (changes in bond length), bending (changes in bond angle), or a combination of both, to infer the presence and type of chemical bonds. Analyses were performed using a Spectrum 100 spectrometer (PerkinElmer, USA) with a scanning range of 1450–4000 cm^{-1}. Solid samples were finely ground and analyzed either in powder form or as potassium bromide (KBr) pellets to ensure spectral accuracy. FTIR provided insights into the alteration of soil chemistry induced by hydrocarbon contaminants and bentonite stabilization.

3. RESULTS AND DISCUSSION

3. 1. Energy Dispersive X-ray Spectroscopy (EDX) To investigate the elemental composition and morphology of the bentonite used, the EDX spectrum of the bentonite sample was employed, as illustrated in Figure 2. The analysis revealed that oxygen was the most abundant element (45% by weight), followed by silicon (39.4%), aluminum (13.2%), and sodium (2.7%). These findings confirm the mineralogical signature of bentonite, characterized by high silica and alumina content, consistent with the presence of montmorillonite as the dominant mineral phase. Aluminum is an essential

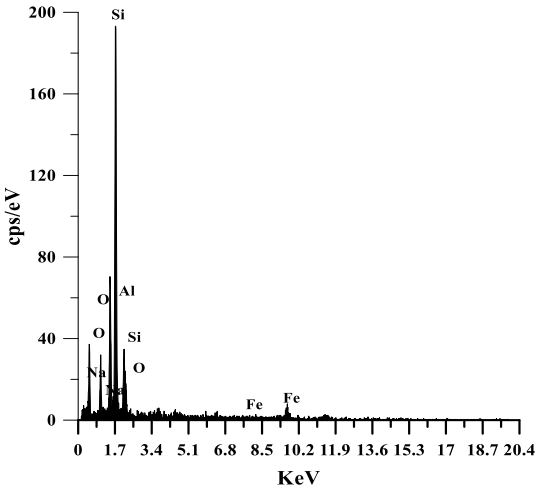

Figure 2. EDX pattern of bentonite

component of the tetrahedral/octahedral sheets in montmorillonite, contributing to the cation exchange capacity (CEC).

3. 2. Compaction Characteristics of Contaminated Specimens Figures 3 and 4 presents the results of the standard compaction tests conducted on soil specimens containing various BSR (0, 0.2, 0.4, and 0.6), with varying levels of diesel and benzene contamination, respectively. As illustrated, at a constant bentonite content, increasing the proportion of hydrocarbon contaminants results in a noticeable increase in MDD and a corresponding decrease in OMC.

This trend can be attributed to the lubricating effect of diesel and benzene, both of which exhibit relatively low polarity and high viscosity. As the contamination level increase, a greater fraction of the soil surface becomes coated with hydrocarbons. This coating reduces interparticle friction and facilitates particle slippage and rearrangement, leading to a denser particle packing. This effect, indirectly evidenced by the observed increase in MDD and decrease in OMC, is consistent with previous studies (32, 38) that reported reduced void ratio and pore volume in TPH-contaminated soils.

Moreover, both diesel and benzene are hydrophobic in nature, forming a nonpolar film around soil particles that inhibits water-soil interaction. This hydrophobic barrier limits the soil's water absorption capacity, thereby reducing the amount of moisture required to achieve optimum compaction. The combination of reduced interparticle resistance and decreased water demand results in a compaction curve that shifts toward higher densities and lower moisture contents compared to uncontaminated conditions.

3. 3. Influence of NAPLs and BSR on Compaction Behavior The interaction between soil particles and NAPLs alters the physicochemical structure of the soil matrix, particularly through the reduction of the diffuse double layer surrounding clay minerals. This contraction of the double layer brings particles closer together, thereby enhancing intergranular contact under a given compaction effort. As a result, the MDD increases due to improved particle coherence—an effect previously reported by Meegoda and Ratnaweera (40) and Al-Sanad et al. (41).

The findings of the present study demonstrate that increasing hydrocarbon contamination leads to a consistent reduction in OMC, accompanied by an increase in MDD, which aligns well with earlier research. The lubricating properties of hydrocarbons, particularly diesel and benzene, contribute to this outcome by reducing interparticle friction and facilitating denser packing during compaction. Furthermore, the hydrophobic nature of these contaminants restricts water-soil interaction, lowering the amount of water needed to reach optimum compaction.

At a constant contamination level, increasing the bentonite content results in a further increase in MDD, suggesting that the addition of bentonite enhances soil structure through its high specific surface area and water absorption capacity. Consequently, the OMC also increase, as more water is required to hydrate the bentonite particles and achieve the desired compaction response.

Notably, the observed rate of change in compaction parameters was more pronounced in diesel-contaminated samples compared to those treated with benzene. This can be attributed to the higher viscosity of diesel, which intensifies its lubricating effect—a trend corroborated by previous studies such as those by Hanaei et al. (29), Shin and Das (42). Similarly, Kermani and Ebadi (43) observed that increasing hydrocarbon content from 4% to 12% led to a progressive increase in dry density and concurrent decrease in moisture content. However, some studies have reported contrasting behavior; for instance, Al-Sanad et al. (41) noted a decrease in dry density at contamination levels between 4% and 6%. These variations underline the complex interplay between contaminant type, viscosity, and soil mineralogy in governing compaction characteristics.

Based on the results, both diesel and benzene increase MDD and reduce OMC of soil mixtures, but benzene shows a significantly weaker effect. At the concentration of 200–250 g/kg dry soil, MDD increases less in benzene-contaminated soils due to lower polarity, and lighter molecular structure. Increasing BSR higher volatility, content mitigates both effects, but it is more effective against diesel than benzene. This is likely due to bentonite's higher affinity for heavier hydrocarbons like diesel. Overall, benzene impairs compaction more severely, necessitating enhanced stabilization strategies for affected soils.

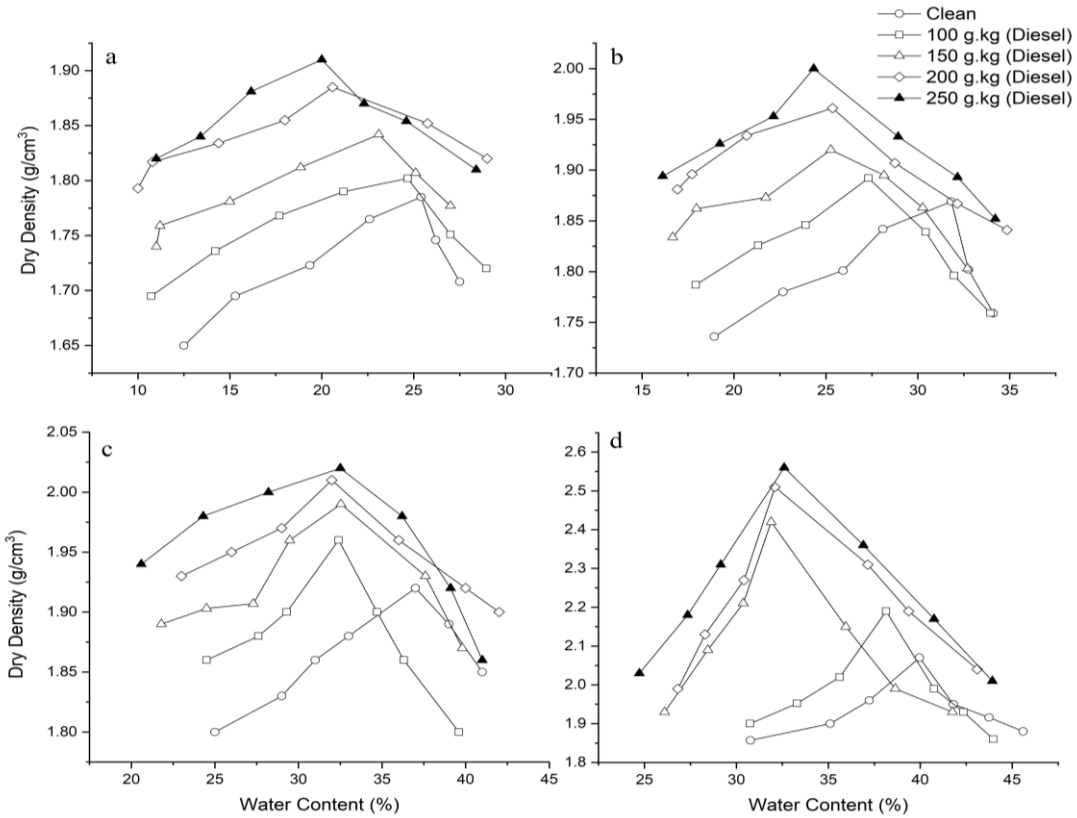

Figure 3. The influence of diesel concentration on dry density curves and water content in soil mixture with different BSR a) 0, b) 0.2, c) 0.4, and d) 0.6

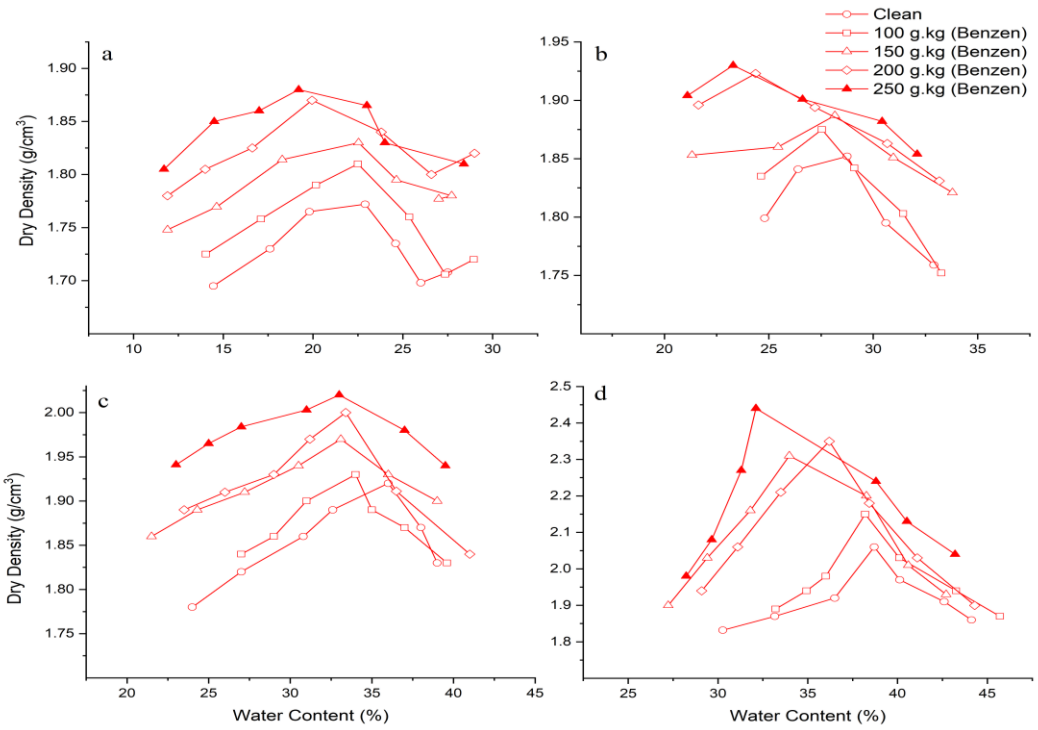

Figure 4. The influence of benzene concentration on dry density curves and water content in soil mixture with different BSR a) 0, b) 0.2, c) 0.4, and d) 0.6

3. 4. Variation in Soil Cohesion and Internal Friction Angle Figures 5 and 6 present the variation in soil cohesion (c) and internal friction angle (ϕ) with different BSR and contaminant concentration.

The test results indicate that cohesion in both diesel- and benzene-contaminated soils increases with increasing BSR. At BSR = 0.0, cohesion values are minimal, ranging from 1 to 9 kPa depending on contaminant type and concentration. However, as the BSR increases to 0.6, cohesion sharply increases and reaches between 45 and 75 kPa. The cohesion gain is attributed to the interparticle binding effect of bentonite, which promotes electrochemical attractions and reduces void ratio. Overall, cohesion was observed to increase with bentonite addition, due to the intrinsic cohesive properties of bentonite and its high viscosity and surface area, which contribute to the formation of interparticle bonds (44). Conversely, increasing the concentration of diesel or benzene contamination led to a decline in cohesion. On average, sand–bentonite mixtures contaminated with NAPLs exhibited a 45% increase in cohesion compared to clean sand, although this gain diminished with increasing contaminant concentration. The observed reduction in cohesion due to hydrocarbon exposure is likely the result of diminished cation exchange capacity, replacement of adsorbed water by contaminant molecules, and a reduction in the soil's effective specific surface area (38). In essence, while bentonite enhances cohesion, NAPLs tend to offset this effect, particularly at higher concentrations.

These trends are consistent with those reported by Mohammadi and Ebadi (44), who found that at a fixed bentonite level, increasing NAPL content reduces the angle of internal friction while marginally increasing or stabilizing cohesion. Similarly, Shin and Das (42) and Khamehchiyan et al. (38) reported significant reductions in ϕ in poorly graded or silty sands subjected to oil contamination. The extent of changes in both ϕ and c appears to be strongly influenced by the viscosity of the NAPL contaminant. More viscous fluids, such as diesel, exhibit a stronger lubricating effect and promote more significant reductions in internal friction angle, a finding supported by Khosravi et al. (45) and other researchers.

At BSR=0, diesel consistently exhibit higher cohesion than benzene. This pattern can be explained by the viscous, adhesive nature of diesel, which coats soil particles and enhances apparent cohesion, whereas benzene (with more volatile and less interactive) has a weaker bonding effect. Similar this results Taheri et al. (46) observed diesel contamination increased cohesion in sand–bentonite soil due to flocculation and particle agglomeration. In contrast, Hanaei et al. (29) found that the effect of benzene on cohesion was more less intense and primarily dependent on bentonite content.

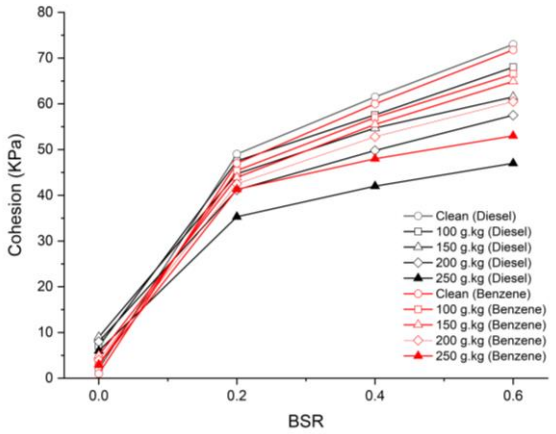

Figure 5. Cohesion function variation of soil mixture contaminated with diesel and benzene at different BSR

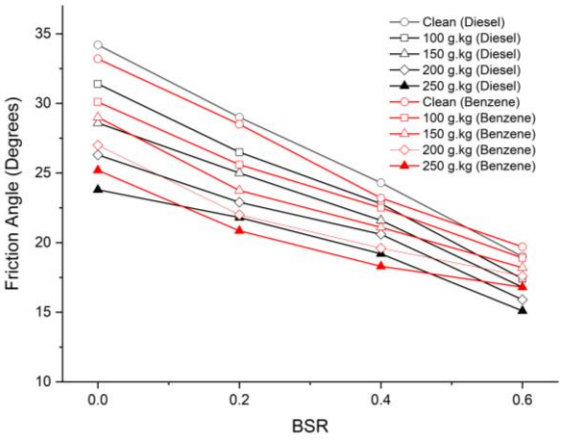

Figure 6. The change of the internal friction angle in diesel and benzene contaminated soil mixture at different BSR

3. 5. Permeability Response to NAPL Contamination and Bentonite Content Figure 7 illustrates the variation in the coefficient of permeability (k) for sand–bentonite mixtures subjected to diesel and benzene contamination at different concentrations of various BSR (0, 0.2, 0.4, and 0.6). The data indicate a clear decreasing trend in hydraulic conductivity with increasing proportions of both NAPL contaminants and bentonite specifically, for specimens contaminated with 200 g benzene/kg dry soil, the permeability was reduced by 31.4%, 61.1%, and 45% at BSRs of 0.2, 0.4, and 0.6, respectively. In comparison, the corresponding reductions for diesel-contaminated specimens were more pronounced—46.2%, 66.8, and 63.5% at the same bentonite contents. These findings suggest that diesel exerts a greater sealing and pore-blocking effect than benzene, which is attributable to its higher viscosity and more significant interaction with soil particles.

Based on the results, the permeability of soil mixtures contaminated with diesel and benzene decreases consistently with increasing contaminant concentration (0–250 g/kg dry soil), and the extent of this reduction is more pronounced with higher bentonite-to-sand ratios (BSR). The most substantial decline in permeability was observed at BSR = 0.6, where the coefficient of permeability dropped below 1×10^{-9} cm/s, indicating nearly impermeable conditions suitable for engineered barrier systems. However, this observation does not contradict the more pronounced percentage reduction in permeability caused by diesel at identical BSRs. The apparent lower absolute permeability in benzene-contaminated soils may stem from deeper infiltration into the bentonite layers, resulting in increased tortuosity and longer flow paths, despite its lower viscosity. Thus, while diesel exhibits stronger pore-blocking due to its viscous nature, benzene's molecular-scale interaction with bentonite contributes to finer microstructural occlusions, leading to distinct permeability behavior. These findings highlight the dual role of bentonite in both reducing hydraulic conductivity and mitigating contaminant transport.

The observed reduction in permeability can be explained by the partial to full filling of pore spaces by NAPL molecules, which obstruct water flow pathways and reduce the effective porosity of the soil matrix. Moreover, the lamellar and swelling characteristics of bentonite amplify this effect by closing off microvoids and increasing soil plasticity. These mechanisms are in agreement with previous studies such as Shin and Das (42) and Al-Aghbari et al. (27), who reported that NAPLs with greater kinematic viscosity cause more severe permeability declines.

Supporting evidence can also be found in earlier works by Khamehchiyan et al. (38)and Hanaei et al. (29), who observed that diesel and benzene contamination in sandy and silty soils significantly reduced permeability, particularly when bentonite was introduced as a sealing agent. These reductions were attributed to decreased pore connectivity and increased interparticle adhesion. Similarly, Sarmadi et al. (32) and Oyediran et al. (47) confirmed that NAPL contamination leads to reduced permeability, lower internal friction angle, and increased apparent cohesion in treated sandy soils.

The role of soil gradation was also emphasized in studies such as Al-Sanad et al. (41), who demonstrated a steady decline in permeability for poorly graded sands exposed to hydrocarbons. Additionally, Khamehchiyan et al. (38) attributed the continued decrease in permeability of silty sands to reduced effective porosity following hydrocarbon exposure.

Collectively, these findings confirm that the permeability reduction in contaminated soil is governed by a combination of fluid viscosity, contaminant content, soil structure, and bentonite-enhanced sealing, all of which are crucial in predicting fluid transport behavior in polluted geotechnical systems.

3. 6. FTIR Analysis Figure 8 depicts the FTIR spectrum of the soil before and after contamination with diesel and benzene for different BSRs (0, 0.2, 0.4, and 0.6). FTIR analysis reveals molecular interactions and functional groups through changes in absorption and transmission intensity. In addition to the higher wavenumber regions, the 400–1450 cm^{-1} fingerprint region was also analyzed to capture key hydrocarbon and clay-related vibrations.

Within the fingerprint region, major peaks were identified at 1030–1056 cm^{-1} (Si–O stretching in bentonite, C–O stretching in alcohols/phenols), 1160–1180 cm^{-1} (C–O–C asymmetric stretching in ethers/esters), 1260–1300 cm^{-1} (COOH bending/CH_2 twisting), 1375–1385 cm^{-1} (CH_3 symmetric bending), and 1450 cm^{-1} (CH_2 bending). Quantitatively, the intensity of these peaks decreased by approximately 60–75 % as the BSR increased from 0 to 0.6, indicating reduced abundance of polar functional groups due to bentonite–LNAPL interactions.

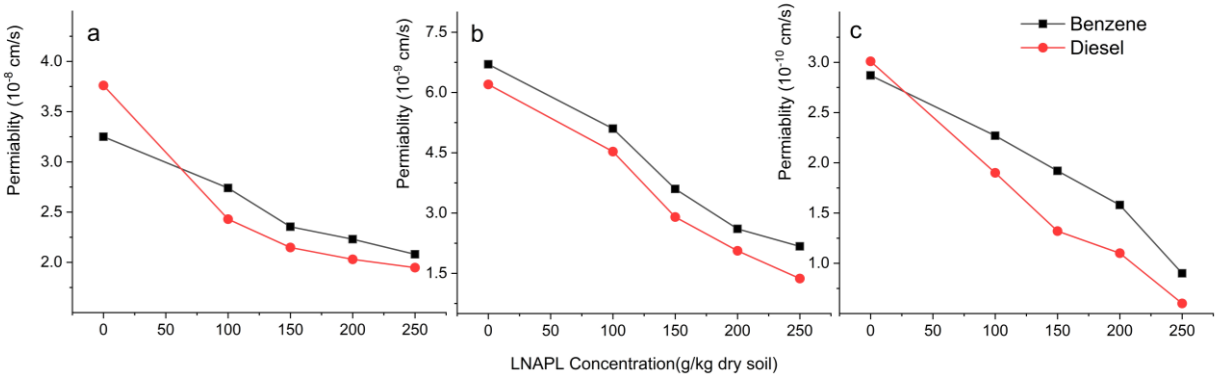

Figure 7. Variation of Permeability contaminated soil with different NAPL and BSR: a) 0.2, b) 0.4, c) 0.6

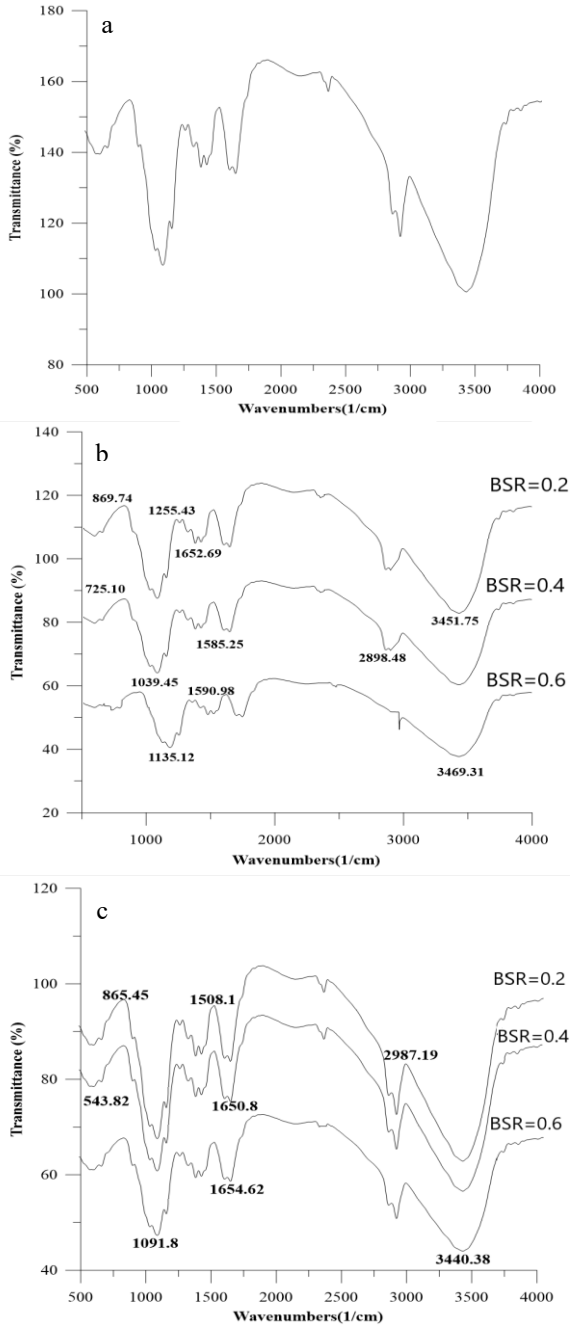

Figure 8. FTIR analysis of soil mixture; a) clean soil b) diesel contaminated soil c) benzene contaminated soil

In the higher wavenumber region, prominent absorption peaks were observed between 1056–1589 cm^{-1} and 2910–3455 cm^{-1}, corresponding to aromatic C=C bending and C–H stretching, confirming the presence of hydrocarbons. Diesel-contaminated soils showed aliphatic C–H stretching bands between 2850 and 3000 cm^{-1}, while benzene-contaminated samples exhibited strong aromatic vibrations around 1600 cm^{-1}. Quantitatively, the absorption peak at 2987 cm^{-1} (aliphatic C–H stretching) decreased from 30 % to 5 % transmittance as BSR increased from 0.2 to 0.6, while the 1600 cm^{-1} peak (aromatic C=C stretching) dropped from 25 % to below 5 %, representing an over 80 % reduction in hydrocarbon-related absorbance. Furthermore, the OH stretching vibration near 1106 cm^{-1} may be related to phenolic groups, suggesting electron resonance effects during hydrocarbon–soil complexation. The absorption at 1300 cm^{-1} likely corresponds to asymmetric carboxyl (COOH) vibrations. As BSR increased, the absorbance intensity of all major peaks declined, further validating bentonite's role in immobilizing contaminants and reducing their mobility.

4. CONCLUSION

A comprehensive research program of laboratory tests was conducted to study the effects of bentonite content on the geoenvironmental behavior of a sandy soil contaminated with different percentages of light non-aqueous phase liquids (LNAPLs). For this purpose, different concentrations (100, 150, 200, and 250 g LNAPLs/kg dry soil) for various BSR (0, 0.2, 0.4, and 0.6) were subjected to standard compaction tests, direct shear tests (to determine the internal friction angle and cohesion), permeability tests, and FTIR. For a constant amount of bentonite, with the increase of the contamination, the MDD increased and the OMC decreased. According to the results, larger amounts of bentonite resulted in higher MDD and OMC of the soil. Specifically, at a contamination level of 250 g/kg, MDD increased by 5.4% for diesel and 3.8% for benzene relative to the clean sample. The internal friction angle decreased by 30.7% for diesel and 19.4% for benzene, while cohesion increased by 24.9% and 28.3%, respectively. These quantitative differences confirm that diesel generally induced more pronounced changes in geotechnical properties than benzene. At a constant BSR, higher contamination leads to lower internal friction angles and decreasing cohesion. Increasing the NAPL concentration resulted in a reduction in the internal friction angle, while the cohesion of the soil samples showed a similar decrease that highlights the lubricating effect of NAPL on interparticle friction and the simultaneous decrease of apparent cohesion due to the covering of the soil surface by NAPL and the change in the electronic double layer. The results of the permeability test revealed that, for all BSR, the permeability decreased with increasing of NAPL concentration. For different BSR, the minimum permeability was observed at BSR=0.6. While the absolute minimum permeability was achieved at BSR = 0.6, the results demonstrated that BSR = 0.4 provides the most balanced combination of high MDD, low permeability (between 1×10^{-9} – 7×10^{-9} cm/s), high

cohesion, and acceptable internal friction angles. These characteristics, combined with better compactability and lower cost, make BSR = 0.4 more practical for engineering applications than BSR = 0.6. Notably, the rate of permeability reduction was dependent on both the contaminant concentration and the physicochemical properties, particularly the viscosity of diesel and benzene.

5. REFERENCES

1. Sasivongpakdi A, Lee J-Y, Bharadwaj H, Keener TC, Barth EF, Clark PJ, et al. Evaluation of a sustainable remediation option: Beneficial reuse of petroleum-contaminated sediment as an energy source. Journal of the Air & Waste Management Association. 2012;62(11):1277-84.
2. Streche C, Cocârţă DM, Istrate I-A, Badea AA. Decontamination of petroleum-contaminated soils using the electrochemical technique: remediation degree and energy consumption. Scientific Reports. 2018;8(1):3272.
3. Adams R, Guzmán-Osorio F, Domínguez-Rodríguez V. Field-scale evaluation of the chemical–biological stabilization process for the remediation of hydrocarbon-contaminated soil. International Journal of Environmental Science and Technology. 2014;11(5):1343-52. https://doi.org/10.1007/s13762-013-0321-1
4. Qv M, Bao J, Wang W, Dai D, Wu Q, Li S, et al. Bentonite addition enhances the biodegradation of petroleum pollutants and bacterial community succession during the aerobic co-composting of waste heavy oil with agricultural wastes. Journal of hazardous materials. 2024;462:132655. 10.1016/j.jhazmat.2023.132655
5. Li Y-T, Li D, Lai L-J, Li Y-H. Remediation of petroleum hydrocarbon contaminated soil by using activated persulfate with ultrasound and ultrasound/Fe. Chemosphere. 2020;238:124657. https://doi.org/10.1016/j.chemosphere.2019.124657
6. Gupta PK, Yadav BK. Bioremediation of non-aqueous phase liquids (NAPLS) polluted soil and water resources. Environmental Pollutants and their Bioremediation Approaches CRC Press, Boca Raton. 2017:241-56.
7. Ossai IC, Ahmed A, Hassan A, Hamid FS. Remediation of soil and water contaminated with petroleum hydrocarbon: A review. Environmental Technology & Innovation. 2020;17:100526. https://doi.org/10.1016/j.eti.2019.100526
8. Wiedemeier TH, Rifai HS, Newell CJ, Wilson JT. Natural attenuation of fuels and chlorinated solvents in the subsurface: John Wiley & Sons; 1999.
9. Wenhui L, Hepeng Z, Hongliang L, Jiale C, Hengxiao Y, Qiang S. Characterization of Water Distribution Characteristics in Response to Light Non-Aqueous Phase Liquids Migration Processes. Polish Journal of Environmental Studies. https://doi.org/10.15244/pjoes/196735
10. Sharma HD, Reddy KR. Geoenvironmental engineering: site remediation, waste containment, and emerging waste management technologies: John Wiley & Sons; 2004.
11. Nierwinski HP, Sosnoski J, Heidemann M. Evaluation of strength and durability of compacted bauxite tailings treated with cement. Clean Technologies and Environmental Policy. 2025:1-10. https://doi.org/10.1007/s10098-025-03212-x
12. Mitchell J, Soga K. Fundamentals of soil behavior. 2005.
13. Lake CB, Rowe RK. The 14-year performance of a compacted clay liner used as part of a composite liner system for a leachate lagoon. Geotechnical & Geological Engineering. 2005;23(6):657-78. https://doi.org/10.1007/s10706-004-8815-8
14. Akbarpour A, Kebria DY. Enhanced remediation of naphthalene from aqueous solutions using synthesized organoclay: characterization, mechanisms, and isotherms. Environmental Monitoring and Assessment. 2025;197(2):152. https://doi.org/10.1007/s10661-024-13533-x
15. Ghavami M, Yousefi Kebria D, Javadi S, Ghasemi-Fare O. Cement-organobentonite admixtures for stabilization/solidification of PAH-contaminated soil: A laboratory study. Soil and Sediment Contamination: An International Journal. 2019;28(3):304-22. https://doi.org/10.1080/15320383.2018.1564734
16. Tamadon Ghareghie H, Yazdi M, Yousefi Kebria D, Aminirad H. Analysis of dense non-aqueous phase liquid contaminants effects on soil permeability by response surface methodology. Iranica Journal of Energy & Environment. 2022;13(2):141-50. https://doi.org/10.5829/ijee.2022.13.02.05
17. Nasrollahpour S, Kebria DY, Nehdi ML, Tanhadoust A, Ghavami M. Remediation of NAPL-contaminated brackish water by synthesized organoclay: Experimental analysis and BNN predictive model. Journal of Hazardous, Toxic, and Radioactive Waste. 2023;27(4):04023028. https://doi.org/10.1061/JHTRBP.HZENG-1212
18. Tekyeh S, Amini Rad H, Kebria DY. Simultaneous removal of salt and dissolved petroleum compounds by a two-stage process: spiral wound capacitive deionization three-dimensional electro-Fenton. Environmental Science and Pollution Research. 2025;32(15):9570-92. https://doi.org/10.1007/s11356-025-36254
19. Kebria DY, Khodadadi A, Ganjidoust H, Badkoubi A, Amoozegar M. Isolation and characterization of a novel native Bacillus strain capable of degrading diesel fuel. International Journal of Environmental Science & Technology. 2009;6(3):435-42. https://doi.org/10.1007/BF03326082
20. Sobhan K, Ali H, Riedy K, Huynh H. Evaluating the compressibility behavior of organic soils using laboratory characterization and rapid on-site piezocone penetration testing. International Journal of Geotechnical Engineering. 2007;1(1):9-18. https://doi.org/10.3328/IJGE.2007.01.01.9-18
21. Cheng G, Zhu H-H, Wen Y-N, Shi B, Gao L. Experimental investigation of consolidation properties of nano-bentonite mixed clayey soil. Sustainability. 2020;12(2):459. https://doi.org/10.3390/su12020459
22. de Medeiros AS, da Silva MA. Influence of Emulsion Type and Moisture on the Stiffness of Stabilized Granular Soil. Civil Engineering Journal. 2025;11(6):2282-302. 10.28991/CEJ-2025-011-06-07
23. Zheng L, Mao W, Liu B. Numerical modeling on mechanical properties of cemented phosphogypsum stabilized soil. HighTech Innov J. 2025;6(1):1-20. 10.28991/HIJ-2025-06-01-01
24. Kassem EM, Azzam W, Elsiragy M. On the Use of a Confined Sand Cell to Dampen Induced Machine Vibration in a Stabilized Clay Numerical Study. Civil Engineering Journal. 2025;11(01). 10.28991/CEJ-2025-011-01-018
25. Jacob S, Scalia IV J, Bareither C. Evaluation of Mineral–Bentonite Mixtures to Concurrently Achieve Low Hydraulic Conductivity and High Strength. Geo-EnvironMeet 2025. p. 431-40.
26. Safehian H, Rajabi AM, Ghasemzadeh H. Effect of diesel-contamination on geotechnical properties of illite soil. Engineering Geology. 2018;241:55-63. https://doi.org/10.1016/j.enggeo.2018.04.020
27. Al-Aghbari M, Dutta R, Mohamedzeini Y. Effect of diesel and gasoline on the properties of sands—a comparative study.

International Journal of Geotechnical Engineering. 2011;5(1):61-8. http://dx. doi.org/10.3328/IJGE.2011.05.01.61-68

28. Nasehi SA, Uromeihy A, Nikudel MR, Morsali A. Influence of gas oil contamination on geotechnical properties of fine and coarse-grained soils. Geotechnical and Geological Engineering. 2016;34(1):333-45. http://dx.doi.org/10.1007/s10706-015-9948-7
29. Hanaei F, Sarmadi MS, Rezaee M, Rahmani A. Experimental investigation of the effects of gas oil and benzene on the geotechnical properties of sandy soils. Innovative Infrastructure Solutions. 2021;6(2):61. https://doi.org/10.1007/s41062-020-00433-5
30. Soil ACD-o, Rock. Standard test method for particle-size analysis of soils: ASTM International; 2007.
31. Soil ACD-o, Rock. Standard test methods for specific gravity of soil solids by water pycnometer: ASTM international; 2010.
32. Sarmadi MS, Zohrevand P, Rezaee M. Effect of kerosene contamination on the physical and mechanical properties of sandy soil. Innovative Infrastructure Solutions. 2019;4(1):7. 10.1007/s4106 2-019-0196-1
33. Jahandari S, Mojtahedi SF, Zivari F, Jafari M, Mahmoudi MR, Shokrgozar A, et al. The impact of long-term curing period on the mechanical features of lime-geogrid treated soils. Geomechanics and Geoengineering. 2022;17(1):269-81. 10.1080/17486 025.2020.17397 53
34. Soil ACD-o, Rock. Standard Test Methods for Laboratory Compaction Characteristics of Soil Using Standard Effort (12 400 Ft-lbf/ft3 (600 KN-m/m3)) 1: ASTM international; 2007.
35. ASTM D-. Standard test method for direct shear test of soils under consolidated drained conditions. D3080/D3080M. 2011;3(9).
36. ASTM. ASTM D2434-22, Standard Test Methods for Measurement of Hydraulic Conductivity of Coarse-Grained Soils. American Society Testing of Materials West Conshohocken, PA, USA; 2022.
37. ASTM-D. Standard practice for identification of polymer layers or inclusions by Fourier transform infrared microspectroscopy (FT-IR). ASTM International West Conshohocken; 2018.
38. Khamehchiyan M, Charkhabi AH, Tajik M. Effects of crude oil contamination on geotechnical properties of clayey and sandy soils. Engineering geology. 2007;89(3-4):220-9. https://doi.org/10.1016/j.enggeo.2006.10.009
39. E168-16 A. Standard practices for general techniques of infrared quantitative analysis. ASTM International West Conshohocken; 2016.
40. Meegoda NJ, Ratnaweera P. Compressibility of contaminated fine-grained soils. Geotechnical Testing Journal. 1994;17(1):101-12.
41. Al-Sanad HA, Eid WK, Ismael NF. Geotechnical properties of oil-contaminated Kuwaiti sand. Journal of geotechnical engineering. 1995;121(5):407-12. 10.1061/(ASCE)07339410(1995)121:5(407)
42. Shin E, Das B. Some physical properties of unsaturated oil-contaminated sand. Advances in unsaturated geotechnics2000. p. 142-52.
43. Kermani M, Ebadi T. The effect of oil contamination on the geotechnical properties of fine-grained soils. Soil and Sediment Contamination: An International Journal. 2012;21(5):655-71. https://doi.org/10.1080/15320383.2012.672486
44. Mohammadi A, Ebadi T. Effect of bentonite addition on geotechnical properties of oil-contaminated sandy soil. Journal of Civil Engineering and Construction. 2018;7(4):153-62. https://doi.org/10.32732/jcec.2018.7.4.153
45. Khosravi E, Ghasemzadeh H, Sabour MR, Yazdani H. Geotechnical properties of gas oil-contaminated kaolinite. Engineering Geology. 2013;166:11-6. https://doi.org/10.1016/j.enggeo.2013.08.004
46. Taheri S, Ebadi T, Maknoon R, Amiri M. Predicting variations in the permeability and strength parameters of a sand-bentonite mixture (SBM) contaminated simultaneously with lead (II) and diesel. Applied Clay Science. 2018;157:102-10. https://doi.org/10.1016/j.clay.2018.01.007
47. Oyediran IA, Enya NI. Crude oil effects on some engineering properties of sandy alluvial soil. International Journal of Mining and Geo-Engineering. 2021;55(1):7-10. 10.22059 /ijmge.2020.283051.594815

Persian Abstract

چکیده

نیازهای انرژی برای راهبردهای پاک‌سازی خاک‌های آلوده به فرآورده‌های نفتی از منظرهای زیست‌محیطی و ژئوتکنیکی بسیار حائز اهمیت است .اثربخشی مواد معدنی رسی و سایر مواد تثبیت‌کننده در بهبود ویژگی‌های ژئوتکنیکی خاک‌های ماسه‌ای آلوده به مایعات سبک غیرآبی (LNAPLs) در تحقیقات پیشین تأیید شده است. با این حال، تأثیر همزمان نسبت بنتونیت به ماسه (BSR)، و نوع و غلظت LNAPL بر ویژگی‌های زیست محیطی و ژئوتکنیکی مخلوط خاک، به‌طور جامع بررسی نشده و همچنان به‌درستی شناخته نشده باقی مانده است. در این مطالعه، تاثیر گازوئیل و بنزن با غلظت‌های مختلف (۱۰۰، ۱۵۰، ۲۰۰ و ۲۵۰ گرم به ازای هر ۱۰۰۰ گرم خاک) بر ویژگی‌های ژئومحیطی خاک ماسه‌ای تثبیت‌شده با نسبت‌های مختلف BSR (۰، ۰/۲، ۰/٤ و ۰/٦) به‌صورت جامع ارزیابی شد. نتایج نشان داد که در آزمایش‌های تراکم، چگالی خشک بیشینه (MDD) افزایش و رطوبت بهینه (OMC) کاهش یافته‌اند. همچنین، با افزایش غلظت LNAPLs، کاهش چسبندگی و کاهش زاویه اصطکاک در خاک‌ها مشاهده شد، به‌طوری که تأثیر گازوئیل محسوس‌تر از بنزن بود. با افزایش غلظت هر دو نوع LNAPL، افزایش در چگالی خشک بیشینه و کاهش در رطوبت بهینه نیز گزارش شد. تکنیک‌های تحلیلی شامل FTIR، EDAX و XRD این یافته‌ها را تأیید کردند و بینش‌هایی درباره سازوکارهای نگهداشت آلاینده در خاک‌های ماسه‌ای اصلاح‌شده با بنتونیت ارائه دادند. یافته‌های این تحقیق می‌تواند در طراحی ژئوتکنیکی سازه‌ها بر روی خاک‌های آلوده به LNAPL مورد استفاده قرار گیرد و راهنمایی برای انتخاب روش‌های مناسب پاک‌سازی فراهم آورد.